

InferLine: ML Inference Pipeline Composition Framework

Daniel Crankshaw, Gur-Eyal Sela, Corey Zumar, Xiangxi Mo

Joseph E. Gonzalez, Ion Stoica, Alexey Tumanov

UC Berkeley RISELab

Abstract

The dominant cost in production machine learning workloads is not training individual models but serving predictions from increasingly complex prediction pipelines spanning multiple models, machine learning frameworks, and parallel hardware accelerators. Due to the complex interaction between model configurations and parallel hardware, prediction pipelines are challenging to provision and costly to execute when serving interactive latency-sensitive applications. This challenge is exacerbated by the unpredictable dynamics of bursty workloads.

In this paper we introduce InferLine, a system which efficiently provisions and executes ML inference pipelines subject to end-to-end latency constraints by proactively optimizing and reactively controlling per-model configuration in a fine-grained fashion. Unpredictable changes in the serving workload are dynamically and cost-optimally accommodated with minimal service level degradation. InferLine introduces (1) automated model profiling and pipeline lineage extraction, (2) a fine-grain, cost-minimizing pipeline configuration planner, and (3) a fine-grain reactive controller. InferLine is able to configure and deploy prediction pipelines across a wide range of workload patterns and latency goals. It outperforms coarse-grained configuration alternatives by up to 7.6x in cost while achieving up to 32x lower SLO miss rate on real workloads and generalizes across state-of-the-art model serving frameworks.

1 Introduction

The design of systems for machine learning has largely focused on model training. While training is central to machine learning research, it is only a small part of production machine learning. The dominant cost of production machine learning is inference, the process of

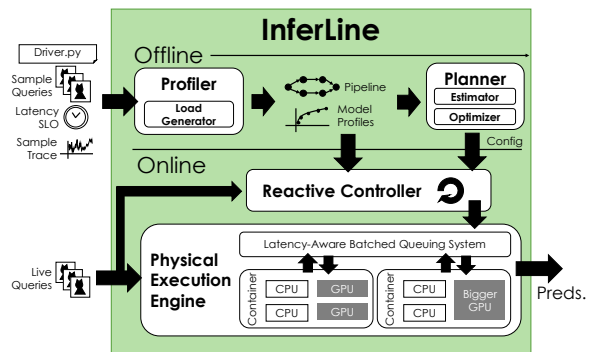


Figure 1: InferLine System Architecture

rendering predictions from trained models. While training systems run periodically on large static datasets, inference systems must run continuously and render predictions within tight end-to-end latency budgets and in response to stochastic and often bursty query arrival processes. Individual predictions may require giga-flops of computation and expensive specialized hardware to meet latency objectives. Indeed, several of the largest industrial users of machine learning were driven by the cost of inference to develop custom hardware [9, 17].

As machine learning matures into an engineering discipline, individual models are being replaced by complex prediction pipelines spanning data transformations, multiple off-the-shelf and custom models, conditional logic, and sophisticated post-processing. Prediction pipelines offer the opportunity to improve accuracy [3, 6], increase throughput [16, 33], and simplify model development [4, 28]. For example, by decomposing complex prediction tasks (e.g., speech translation) into a sequence of simpler prediction tasks (e.g., speech recognition and text translation), established models can be reused to develop new functionality. Moreover, model composition yields the familiar software engi-

neering benefits of modularity by amortizing the development and maintenance cost of models across a wide range of prediction tasks.

While prediction pipelines simplify model development, they substantially complicate inference. Often prediction pipelines will span multiple machine learning frameworks and heterogeneous parallel devices (e.g., GPUs and CPUs) to render a single prediction. The large and growing number of parallel hardware accelerators including multi-core processors, multiple GPU generations (e.g., K80, V100), and specialized accelerators (e.g., TPUs [17]) offer the opportunity to improve throughput and reduce cost. However, to fully leverage the parallel hardware, queries must be processed in batches which can adversely affect latency. Alternatively, the throughput of each component in a pipeline can be increased by replicating the component across multiple parallel devices and distributing queries among them. However, introducing additional devices increases prediction costs. Systems for serving prediction pipelines must navigate a complex trade-off space spanned by latency, throughput, and monetary costs that depend on per-model choices of (a) parallel hardware, (b) per-model batching and (c) number of replicas.

The complexity of navigating this configuration space grows exponentially with each model (stage) in the pipeline and combinatorially in the hardware types, per-model batching options, and replication factor. The need to meet end-to-end latency and throughput requirements fundamentally couples each configuration decision. For example, increasing the batch size of an upstream model to maximize parallelism may tighten the latency requirements of a downstream model and change its optimal hardware configuration. Thus, global reasoning is required to optimally configure a prediction pipeline. Optimal pipeline configuration can have significant consequences on end-to-end latency and cost. For example, optimally configuring a two stage computer vision pipeline resulted in a 7.6X reduction in cost (Sec. §7.1.1).

The complexity of configuring and serving predictions pipelines is exacerbated by the inherently stochastic and bursty nature of real-world prediction query streams. A system that has been aggressively tuned to minimize cost under the assumption of a uniform arrival process can quickly destabilize under realistic bursty workloads resulting in frequent missed latency deadlines. As a consequence, the conventional wisdom in production deployments is to over-provision the pipeline. However, over-provisioning specialized hardware accelerators can be especially costly. In our eval-

uation, we demonstrate that it is possible to dynamically react to observed arrival process burstiness in a *fine-grain*, per-model fashion and maintain high levels of latency SLO attainment while achieving up to 4.2X reduction in cost.

To address these challenges we propose InferLine—a high-performance, general purpose system for provisioning and serving prediction pipelines. InferLine efficiently provisions ML inference pipelines subject to end-to-end latency constraints by *proactively* optimizing and *reactively* controlling per-model configuration in a fine-grain fashion. InferLine combines a *Planner* to optimize the initial pipeline configuration and a *Reactive Controller* to continuously monitor and tune the pipeline configuration at runtime. The *Planner* relies on the end-to-end latency *Estimator* model profiles extracted by the *Profiler* to find a cost minimizing configuration that meets the latency SLO. The prediction pipeline is then served by the physical execution engine with a dynamic, SLO-aware, batched queuing system. The reactive controller monitors the dynamic behavior of the arrival process and extends the fine-grain per-model configuration control at runtime to respond to transient variability in demand.

There are two key enabling observations in the design of InferLine. First, the complex performance characteristics of individual models can be accurately profiled using offline training data and combined to estimate end-to-end pipeline performance across hardware and batching configurations. This end-to-end performance estimator can then be used to both proactively and reactively configure the system to minimize cost and meet latency SLOs. Second, that functional nature of ML inference naturally supports online reactive scaling through replication. The resulting contributions of InferLine are: (1) fine-grain *proactive* pipeline optimizer that minimizes pipeline cost while satisfying given query process and end-to-end latency constraints cost-efficiently, (2) fine-grain *reactive* controller algorithm and system artifact that monitors and adjusts per-model configuration to maintain high SLO attainment at minimum cost. (3) the SLO- and heterogeneity-aware batched queuing layer in the physical execution engine.

We evaluate InferLine across a range of real pipelines using real models subjected to real query traces spanning multiple arrival distributions. We compare InferLine to the state-of-the-art model serving baselines that (a) use coarse-grain proactive configuration of the whole pipeline as a unit (e.g., TensorFlow Serving [32], an open-source model serving system developed at Google), and (b) state-of-the-art coarse-grain reactive

mechanisms [10]. Even with the benefit of InferLine’s deadline-aware, dynamic batching queuing layer, we find that InferLine significantly outperforms the baselines by a factor of up to 7.6X on cost, while maintaining the highest level of latency SLO attainment.

2 Prediction Pipelines

Prediction pipelines combine multiple machine learning models and data transformations to support complex prediction tasks [29]. For instance, state-of-the-art visual question answering services [1, 21] combine natural language models for question parsing with computer vision models to answer to the question.

Prediction pipelines simplify model development by allowing model developers to reuse models [34] that have been pre-trained on large well studied benchmark datasets or developed internally and used across the organization. In many cases, a single model (e.g., ResNet152 [13]) may be re-used as a feature function for a wide range of prediction tasks [15]. The output of these feature functions are then used as inputs to more robust and easier to train models (e.g., linear models). By avoiding the need to go through the costly model design and training process, this form of model reuse can substantially accelerate application development.

A prediction pipeline can be formally encoded as a directed acyclic graph (DAG) where each vertex corresponds to a model (e.g., a mapping from images to a list of objects in the image) or some other more basic data transformation (e.g., extracting key frames from a video) and each edge represents a data flow. In this paper we study several (Figure 2) common prediction pipelines. The photo analysis pipeline, consists of basic image pre-processing (e.g., cropping and resizing) followed by image classification using a deep neural network. The video monitoring pipeline was inspired by [35] and uses an object detection model to identify vehicles and people and then performs subsequent analysis including vehicle and person identification and license plate extraction on the relevant any images. The social media prediction pipeline translates and categorizes posts based on both text and linked images by combining computer vision models with multiple stages of language model to identify the source language and translate the post if necessary. Finally, the TF Cascade pipeline, combines fast and slow models implemented fully in TensorFlow and invokes the slow model only when the fast model is uncertain about its prediction.

In both the social media and TF cascade pipelines, a subset of models are invoked based on the output of earlier models in the pipeline. This is common pattern appears in bandit algorithms [3, 20] used for model per-

sonalization as well as more general cascaded prediction pipelines [2, 12, 22, 30]. Capturing this conditional execution (corresponding to a sub-graph of the prediction pipeline DAG) is critical when provisioning and executing these pipelines.

2.1 Systems Challenges

Prediction pipelines present categorically new challenges for the design and provisioning of prediction serving systems. In this section we discuss the key challenges around parallel hardware accelerators, pipeline level parallelism, the combinatorial configuration space, messaging and queuing delays, and the complexities of meeting tight latency service level objectives (SLOs) under bursty stochastic query loads.

Parallel Hardware Accelerators. Many machine learning models can be computationally intensive with substantial opportunities for parallelism. A single deep neural network may have many stages that can benefit from parallel hardware. In some cases, this parallelism can result in orders of magnitude improvements in throughput and latency. For example, in our experiments we found that TensorFlow can render predictions for the relatively large ResNet152 neural network at 0.6 queries per second (QPS) on a CPU and at 191 QPS on an NVIDIA Tesla V100 GPU (a 300x difference in throughput). However, not all models benefit equally from hardware accelerators. For example, many widely used classical models (e.g., decision trees [7]) can be difficult to parallelize on GPUs.

Determining the Per-Model Batchsize. In many cases, to fully utilize the available parallel hardware, queries must be processed in batches (e.g., ResNet152 required a batch size of 32 to maximize throughput on the V100). However, processing queries in a batch can also increase latency. Because most hardware accelerators operate at vector level parallelism, the first query in a batch is not returned until the last query is completed. As a consequence, it is often necessary to set a *maximum* batch size to bound query latency. However, the choice of the maximum batch size depends on the hardware and model and can affect the end-to-end latency of the pipeline.

Pipeline Operator Level Parallelism. In heavy query load settings it is often necessary to leverage parallelism at the level of the pipeline to scale-out individual models and high-fanout stages. Identifying and scaling the bottleneck models is critical to achieving high-throughput at low cost. Pipelines with high-fanout stages (e.g., ensembles of models) can often be accelerated by di-

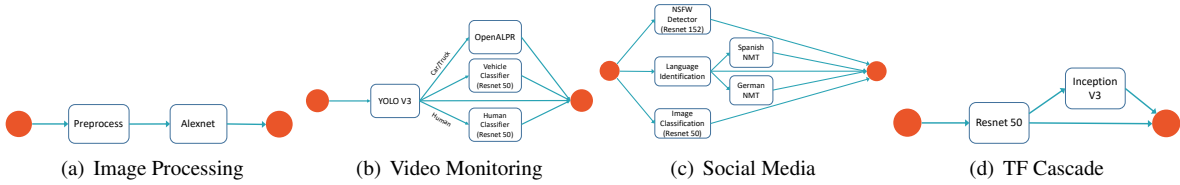


Figure 2: Example pipelines for evaluation. We evaluate InferLine on four prediction pipelines that span a wide range of models, control flow, and input characteristics.

viding compute resources across parallel paths in the pipeline. However, the optimal placement of resources depends heavily on the performance characteristics of each model and the optimal choice of batch size. Furthermore, as we scale the compositions of models, we quickly discover that individual components scale differently, an effect that can be amplified by the use of conditional control flow within a pipeline causing some components to be queried more frequently than others.

Combinatorial Configuration Space. Allocating parallel hardware resources to a single model presents a complex model dependent trade-off space between cost, throughput, and latency. This trade-off space grows exponentially with each model in a prediction pipeline. Decisions made about the choice of hardware, batching parameters, and replication factor at one stage of the pipeline can affect choices at subsequent stages. For example, trading latency for increased throughput on one model reduces the latency budget of subsequent models in the pipeline and as a consequence the feasible hardware configurations.

Distributed Messaging and queuing. Because prediction pipelines span multiple hardware devices that run at different speeds and batch sizes, buffering in the form of queues is needed between stages. However, queuing adds to the latency of the system. Therefore queuing delays, which depend on the arrival process and system configuration, must be considered when provisioning the end-to-end pipeline.

Bursty, Stochastic Query Arrival Process. Finally, prediction serving systems must respond to bursty, stochastic query streams while meeting tight latency objectives. At a high-level these stochastic processes can be characterized by their average arrival rate λ and their coefficient of variation, a dimensionless measure of dispersion defined by $CV = \frac{\sigma^2}{\mu^2}$, where σ and $\mu = 1/\lambda$ are the standard-deviation and mean of the query inter-arrival time. Processes with higher CV have higher variability and often require additional over-provisioning to meet query latency requirements. However, over-provisioning an entire pipeline on specialized hardware

can be prohibitively expensive. Therefore, it is critical to be able to identify and provision the hotspots in a pipeline to accommodate the bursty arrival process. Finally, as the workload changes, we need mechanisms to quickly detect and scale up (or down) replicas of individual stages in the pipeline.

3 System Design and Architecture

In this section, we provide a high-level overview of the main system components in InferLine (Fig. 1): the *Profiler*, the *Planner*, the *Physical Execution Engine*, and the *Reactive Controller*. The *Profiler* and *Planner* are run offline and used to estimate model performance characteristics and optimally provision and configure the system for a given sample workload and latency SLO. The *Physical Execution Engine* then provisions model container resources according to the configuration produced by the *Planner* and hosts pipeline for serving. The *Reactive Controller* monitors and detects unexpected changes in the arrival process and reactively adjusts the configuration to meet the latency SLO.

3.1 Pipeline Specification

InferLine serves prediction pipelines by processing a stream of queries submitted by clients while dynamically adjusting its configuration to meet the specified end-to-end latency constraints while minimizing cost.

Prediction pipelines in InferLine are implemented as a stateless driver program that takes as input a query and returns a prediction. Within this driver function, developers interleave application-specific code executed in the driver with asynchronous RPC calls to models hosted in InferLine. This flexible programming model addresses the fundamental need for an expressive mechanism to compose models, control flow, and data transformations within a prediction pipeline.

To support user defined logic and flexible model composition, InferLine allows users to specify their pipeline in a fully featured Python function. However, in order to support query planning and scale-out model execution on different hardware accelerators, InferLine needs

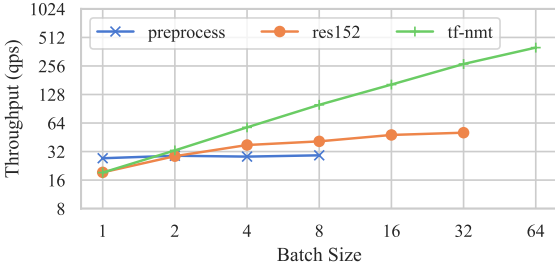


Figure 3: Example Model Profiles. The preprocess model has no internal parallelism and cannot utilize a GPU. Thus, it sees no benefit from batching. Res152 (image classification) & TF-NMT(text translation model) benefit from batching on a GPU. a way to capture statistics about the pipeline call graph and move model invocation out of the driver process.

InferLine exposes a Python client API backed by a C++ RPC client that issues queries to the InferLine serving system. To query an individual model within the pipeline, the driver program makes an RPC request to InferLine specifying the model name and providing the input. The RPC request is then dispatched to one of the containers (see §3.6) which serves that model. This RPC request is asynchronous and returns a future so that pipelines can evaluate multiple models in parallel. Finally, the futures are used to extract statistics about the relative frequency of model invocations used for planning.

3.2 Profiler

The *Profiler* takes a pipeline driver and a sample query trace and extracts the logical pipeline structure as a directed acyclic graph (DAG) of data and control flow dependencies between models. The *Profiler* also creates a performance profile of each of the component models in the pipeline as a function of model batch size and hardware.

InferLine uses runtime tracing to infer the pipeline structure directly from the user-provided driver program by executing a sample set of queries. The profiler evaluates the driver on each of the sample queries, tracing the lineage of each query as it traverses the pipeline through the RPC system. The union of all the traced query lineage graphs forms a single pipeline graph. We track the frequency of a query visiting each model. This frequency represents the conditional probability that a model will be evaluated given a query entering the pipeline independent of the behavior of any other models, which we refer to as the *scale factor* s of the model. The scale factor is used by the *Estimator* to estimate the effects of conditional control flow on latency (§3.4).

The profiler captures model throughput as a function

of hardware type and maximum batch size to create per-model performance profiles. An individual model configuration corresponds to a specific value for each of these parameters. Both the batch size and the hardware type provide mechanisms for exploiting a model’s parallelism and offer diminishing returns. The profiler exploits this property in two ways. First, profiling a single replica is sufficient, as the models are side-effect free and scale horizontally. Second, batch sizes are considered in powers of 2 to detect maximum performance without the need for linear search.

While we ensure that models have exclusive access to the CPUs and GPUs allocated to them in their resource bundles there are still sources of kernel level contention (e.g., memory allocation or GPU calls) that can reduce model throughput on a heavily loaded multi-core machine. To ensure that InferLine’s configurations are feasible on fully utilized machines, we simulate a load on the machine by running additional replicas of the model on the available compute resources during profiling, rather than profiling on an idle machine.

3.3 Planner

The *Planner* is responsible for the initial pipeline configuration subject to the end-to-end latency SLO and the specified arrival process. It sets the three control parameters for each model in the pipeline using a globally-aware, cost-minimizing optimization algorithm. The *Planner* uses the model profiles extracted by the *Profiler* to select cost-minimizing steps in each iteration while relying on the *Estimator* to check for latency constraint violations. We cover the algorithm in §4.

3.4 Estimator

The *Estimator* is responsible for rapidly estimating the end-to-end latency of a given pipeline configuration for the sample query trace. It takes as input a pipeline configuration, the individual model profiles, and a sample trace of the query workload, and returns accurate estimates of the latency for *each query* in the trace. The *Estimator* is implemented as a continuous-time, discrete-event simulator [5], simulating the entire pipeline, including queuing delays. The simulator maintains a global logical clock that is advanced from one discrete event to the next with each event triggering future events that are processed in temporal order. Because the simulation only models discrete events, we were able to faithfully simulate hours worth of real-world trace in hundreds of milliseconds.

3.5 Reactive Controller

The *Reactive Controller* monitors the dynamic behavior of the arrival process as well as the instantaneous end-to-end system performance to adjust per-model control parameters and maintain high SLO attainment at low cost. More specifically, the *Reactive Controller* continuously monitors the current arrival curve [19] to detect deviations from the planned arrival process at different timescales simultaneously. By analyzing the timescale at which the deviation occurred, the *Reactive Controller* is able to take appropriate mitigating action to ensure that SLOs are met without unnecessarily increasing cost. We discuss the *Reactive Controller* in more detail in §5 and provide an extensive analysis of its behavior under different arrival processes in §7.2.

3.6 Physical Execution Engine

Similar to [8, 14], the *Physical Execution Engine* adopts a distributed microservice architecture with an RPC interface, allowing models to dictate their environment dependencies and enabling the serving system to be distributed across a cluster of heterogeneous hardware. Each model replica is hosted in a separate model container and queried via RPC.

The *Physical Execution Engine* interposes a latency-aware batched queuing system to tightly control how queries are distributed among model replicas. All requests to a model are placed in a unique centralized queue for all replicas of that model. To ensure that InferLine is always processing the queries that will expire first, InferLine uses earliest deadline first (EDF) priority queues.

When a model replica is ready to process a new batch of inputs, it requests a new batch from the centralized queue for that model. The size of the batch is bounded above by the maximum *batch size* for the model as configured by the *Planner*. By employing a pull-based queuing strategy and imposing a maximum batch size, InferLine places an upper bound on the time that a query will spend in the model container itself after leaving the queue. Furthermore, unlike randomized load-balancing the deterministic centralized queuing policy allows the *Estimator* to accurately estimate queuing latencies.

4 The Proactive Planner Algorithm

At a high-level, the *Planner* is a cost-minimizing algorithm that iteratively optimizes the pipeline configuration subject to the latency constraints. The *Planner* algorithm can be divided into two phases. In the first phase, it finds a feasible but expensive configuration of

the pipeline that meets the latency constraint to serve as an initial configuration. In the second phase, the planner greedily modifies the configuration to reduce the cost while using the *Estimator* to ensure that each new configuration does not violate the latency SLO on the sample query trace. The algorithm has converged when it can no longer make any cost reducing modifications to the configuration without violating the latency SLO.

Initialization: To generate the initial configuration, the *Planner* first greedily minimizes pipeline latency by configuring each model to use the most expensive available hardware and setting the batch size to one. If the service time of the pipeline under this configuration is greater than the SLO then the latency constraint is infeasible given the available hardware and the planner terminates. It then iteratively determines the *throughput bottleneck* in the pipeline and increases that model’s replication factor until the model is no longer a bottleneck. Once the *Estimator* indicates that the latency constraint is met, this stage terminates.

Cost-Minimization: In each iteration of the cost-minimizing process, the *Planner* considers three candidate modifications for each model: increase the batch size, decrease the replication factor, or downgrade the hardware. It evaluates each of these actions on every model in the pipeline, eliminating candidate actions that violate the latency SLO according to the *Estimator*.

The batch size is increased by factors of two to match the profiled batch sizes. Increasing the batch size only affects throughput and does not affect cost, and will therefore only be chosen if no other actions are feasible. In contrast, decreasing the replication factor directly reduces costs by removing container replicas.

The action of downgrading hardware is substantially more complex than the other two actions, as the batch size and replication factor for the model must be re-evaluated to account for the differing batching behavior of the new hardware. For example, downgrading from a GPU to a CPU eliminates a significant amounts of parallel computation and so retaining the batch size from the GPU can lead to a large increase in latency. It is therefore often necessary to reduce the batch size and increase in replication factor to find a feasible pipeline configuration. However, the reduction in hardware price can occasionally compensate for the increased replication factor. For example, in Fig. 9, the steep decrease in cost when moving from an SLO of 0.1 to 0.15 can be largely attributed to downgrading the resource allocation of a language identification model from a GPU to a CPU.

To evaluate a resource allocation downgrade on a

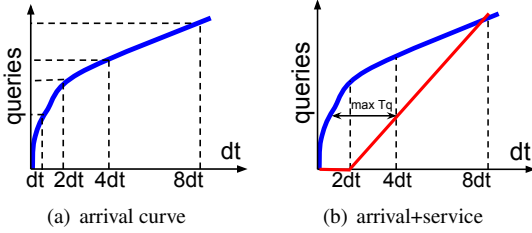


Figure 4: InferLine *Reactive Controller* tracks the arrival curve (blue) at runtime. X-axis represents Δt with exponentially increasing look-back time window. Y-axis counts queries arrived in the past Δt time window. A well-behaved arrival process doesn't exceed its provisioned arrival curve at any point. The service curve (red) represents the number of queries that the system is provisioned to service in Δt . The maximum horizontal distance between the arrival and service curves is the maximum expected queuing delay T_q . *Reactive Controller* heuristic algorithm fits a service curve to the observed arrival curve to cap T_q .

model, we first fix the configurations of the other models in the pipeline and re-perform the initial configuration generation phase. The planner then performs a localized version of the overall cost-minimizing algorithm to find the batch size and replication factor for the model on the newly downgraded resource allocation needed to reduce the cost of the previous configuration. If there is no cost reducing feasible configuration than the hardware downgrade action is rejected.

The *Planner* terminates when no actions can be taken without violating one of the invariants, and returns the latest configuration as the final, cost-minimizing one.

5 Reactive Controller Algorithm

The reactive controller is responsible for runtime monitoring and adjustment of the inference pipeline configuration to ensure robustness to the unforeseen dynamics of the arrival process. Recall that the arrival process may experience bursts, causing transient overloads, as well as unexpected changes in the mean arrival rate. The reactive controller algorithm detects *when* to take reactive action, *which* model an action should be applied to, and *what* reactive action to take. InferLine's reactive algorithm leverages techniques from network calculus and queuing theory.

Detecting change. Detecting when to take an action is essential to responding quickly while ensuring hysteresis. Recall that the pipeline is provisioned to absorb the burstiness present in the sample query trace (§4). Naive approaches that react to *instantaneous* spikes in the observed arrival rate are too sensitive and would respond to *expected* variability in the inter-arrival pro-

cess. On the opposite extreme, tracking changes in the moving average may help detect changes in the average arrival rate (λ), but will miss unexpected increases in burstiness, which we show are subtle, yet debilitating §7.2.3).

InferLine's *Reactive Controller* maintains a discretized view of the observed arrival curve (Fig. 4). The x-axis marks different time intervals Δt . The y-axis plots the number of queries arriving in the last Δt . We will refer to this as $A(\delta t_i)$. As the system starts, it initializes a static reference arrival curve constructed from the sample arrival process used by the proactive planner. We will refer to it as $A_{max}(\Delta t_i)$. Intuitively, as long as the observed $A(\Delta t_i)$ does not exceed $A_{max}(\Delta t_i)$ for any Δt_i , the observed arrival process is within the provisioned envelop. Conversely, if $A(\Delta t_i)$ exceed $A_{max}(\Delta t_i)$ then a reactive action should be taken. The arrival curve is tracked by maintaining the query count arriving in the past Δt for an exponentially increasing Δt . This mechanism allows us to track changes in the average arrival rate as $A(\Delta t_{max})$ exceeds $A_{max}(\Delta t_{max})$ while also detecting changes in burstiness even when the arrival rate stays constant. This manifests itself as $A(\Delta t_i)$ exceeds $A_{max}(\Delta t_i)$ for the first few bucket sizes i .

The choice of the smallest bucket size Δt_{min} affects the sensitivity of the reactive controller. We draw on intuition from network calculus (Fig. 4(b)) and set the smallest sized bucket to $\sum T_s^m$, which is the sum of estimated service times T_s for all models m on the critical path of a query. T_s can be easily monitored at runtime, but Δt_{min} must be set statically by the *Planner* to calculate $A_{max}(\Delta t_i)$. Recall from §4 that the planner has access to per-model throughput and configures per-model batch sizes. Given this information, we derive $T_s^m = \frac{bs_m}{\mu_m}$, where bs_m is model m 's batch size, and μ_m is its profiled throughput. Thus we set $\Delta t_{min} = \frac{bs_m}{\mu_m}$.

Adding model replicas. Second, the activated reactive algorithm decides what reactive action to take. It takes corrective action limited to changes in the replication factor per-model. Given $A(\Delta t_i)$, we compute $\lambda_{max} = \max_i \left(\frac{A(\Delta t_i)}{\Delta t_i} \right)$, and the new replication factor $k'_m = \frac{\lambda_{max}}{\mu_m}$. In addition, at static planning stage, we calculate $\rho_{max} = \frac{\lambda}{k_m * \mu_m}$, where k_m is the replication factor for model m and μ_m is profiled throughput for model m . This provides maximum model load ρ_{max} at proactive planning stage. We make sure that $k'_m \geq \frac{\lambda_{max}}{\rho_{max} \mu_m}$.

Removing model replicas. The reactive controller tracks the maximum $\lambda = \frac{A(30)}{30}$ over the last 30s, smoothed over a 5 second window. If the reactive controller has not detected any change in $A(\Delta t_i) \forall i$ in the last

10s, it will recalculate k'_m .

6 Experimental Setup

To evaluate InferLine we constructed four representative prediction pipelines (Fig. 2) that span the fundamental model composition patterns. We configure each pipeline with varying input arrival processes and latency budgets, and then evaluate the latency SLO attainment and pipeline cost-effectiveness under a range of both synthetic and real world workloads. We characterize the synthetic workloads by their mean request rate (λ) and coefficient of variation (CV), evolving these properties over time within the same workload to add additional dynamicity to the process. We use the same real world traces as those used in [10], and compare the InferLine *Reactive Controller* to the reactive control algorithm described in that work. We evaluate InferLine on the four representative pipelines in Fig. 2, using models trained in a variety of machine learning frameworks including PyTorch [25], TensorFlow [31], DarkNet [26], and OpenALPR [24].

6.1 Baseline Comparison

Current prediction serving systems do not provide first-class support for prediction pipelines with end-to-end latency constraints. Instead, the individual pipeline components are each deployed as a separate microservice to a prediction serving system such as [8, 14, 32] and a pipeline is manually constructed by individual calls to each service. Any performance tuning for end-to-end latency or cost treats the entire pipeline as a single black-box service and tunes it as a whole. Throughout the experimental evaluation we refer to this as the *Coarse-Grained* baseline. We deploy both the InferLine and coarse-grained pipelines on the *Physical Execution Engine* to eliminate any performance variability caused by different underlying execution environments.

We adopt the techniques proposed in [10] for both provisioning and scaling the coarse-grained pipelines. We profile the entire pipeline as a single black box to identify the single maximum batch size capable of meeting the SLO. The pipeline is then replicated as a single unit to achieve the required throughput as measured on the same sample arrival trace using by the InferLine *Planner*. We evaluate two strategies for determining required throughput. *CG-Mean* uses the mean throughput computed over the arrival trace while *CG-Peak* determines the peak throughput in the trace computed using a sliding window of size equal to the SLO. The coarse-grained reactive controller scales the number of pipeline replicas using the scaling algorithm described in [10].

6.2 Physical Execution Environment

We ran all experiments in a distributed cluster on Amazon EC2. In all experiments, the pipeline driver client was deployed on an `m4.16xlarge` instance which has 64 vCPUs, 256 GiB of memory, and 25Gbps networking across two NUMA zones. We used large client instance types to ensure that network bandwidth from the client is not a bottleneck in the experiments. The models were deployed to a cluster of up to 16 `p2.8xlarge` GPU instances. This instance type has 8 NVIDIA K80 GPUs, 32 vCPUs, 488.0 GiB of memory and 10Gbps networking all within a single NUMA node. All instances were running Ubuntu 16.04 with Linux Kernel version 4.4.0.

When deploying a pipeline configured by the *Planner*, the queuing system was deployed on the same instance as the client while the model replicas were randomly distributed across the GPU instances. When deploying the coarse-grained baselines, an entire pipeline replica (queues and all model containers) were deployed to the same instance to minimize network overhead.

6.3 Workload Setup

We generated the traces by sampling inter-arrival times from a Gamma distribution with differing mean β to vary the ingest rate, and coefficient of variation CV to vary the workload burstiness. When reporting performance on a specific workload as characterized by β and CV, a trace for that workload was generated once and reused across all comparison points to provide a more direct comparison of performance. We generated separate traces with the same performance characteristics for profiling and evaluation to avoid overfitting to the sample trace.

To generate synthetic time-varying workloads, we evolve the workload generating function between different Gamma distributions over a specified period of time, the transition time. This allows us to generate workloads that vary in mean throughput, CV, or both, and thus evaluate the performance of the *Reactive Controller* under a wide range of conditions.

In Fig. 7 we evaluate InferLine on traces derived from real workloads studied in [10]. To derive traces from these workloads, we re-scaled the max throughput to 300 QPS, the maximum throughput supported by the coarse-grained pipelines on a 16 node cluster. We then iterated through each of the mean throughputs in the workload and sample from a Gamma distribution with CV 1.0 for 30 seconds. We use the first 15 minutes of the trace for planning, and the remaining 45 minutes for evaluation.

7 Experimental Evaluation

In this section we evaluate InferLine’s end-to-end performance. We start with an all-in validation that a fine-grained approach to heterogeneous ML inference pipeline configuration is needed, both for proactive planning and reactive control (§7.1). We then perform a sensitivity analysis through a series of micro-benchmarks aimed at gauging InferLine’s robustness to the dynamics of the arrival process (§7.2). We find that InferLine is robust to unplanned changes in the arrival rate as well as unexpected inter-arrival bursts. We then perform an ablation study to show that the system benefits from both (a) fine-grain proactive planning and (b) fine-grain reactive control (§7.3). We conclude by showing that InferLine generalizes to other prediction serving systems (§7.4).

7.1 End-to-end Evaluation

We first establish that fine-grain control for InferLine’s proactive (§7.1.1) and reactive (§7.1.2) components outperforms state of the art coarse-grain pipeline-level configuration alternatives in an end-to-end evaluation. InferLine is able to achieve the same throughput at significantly lower cost, while maintaining zero or close to zero latency SLO miss rate. Coarse-grain replication necessarily amplifies the cost of any imbalances in the pipeline.

7.1.1 Proactive fine-grain control

In the absence of a globally reasoning planner (§4), the options are limited to either (a) provisioning for the peak (CG Peak), or (b) provisioning for the mean (CG Mean). We compare InferLine to these two end-points of the configuration continuum across 2 pipelines (Fig. 5 and Fig. 6). InferLine meets latency SLOs at the lowest cost. CG Peak meets SLOs, but at much higher cost, particularly for burstier workloads. And CG Peak is not provisioned to handle bursty arrivals and results in high SLO miss rates. This result is exacerbated by higher burstiness and lower SLO. Furthermore, the InferLine planner consistently finds lower cost configurations than both coarse-grained provisioning strategies and is able to achieve up to a *7.6x reduction in cost* by minimizing pipeline imbalance.

7.1.2 Reactive fine-grain control

InferLine is also able to (1) maintain a negligible SLO miss rate, and (2) reduce cost by up to 4.2x when compared to the state-of-the-art approach [10] when handling unexpected changes in the arrival rate and burstiness. In Fig. 7 we evaluate the *Social Media* pipeline on 2 traces derived from real workloads

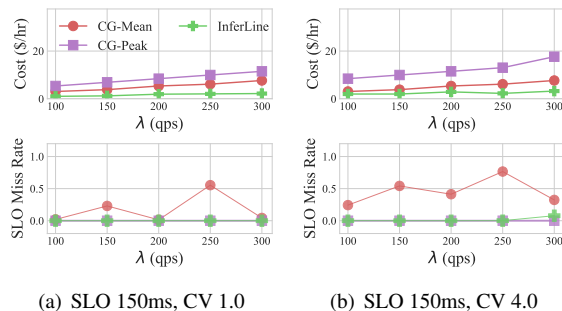


Figure 5: Proactive Planning for Image Processing.

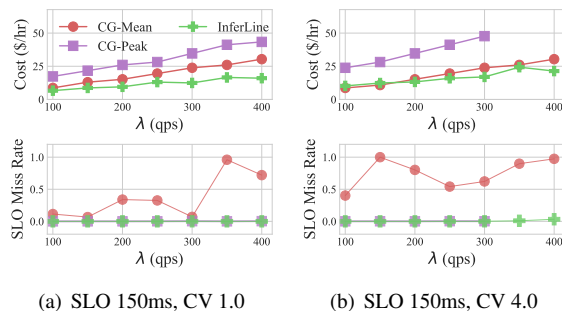


Figure 6: Proactive Planning for Video Monitoring. CG-Peak was not evaluated on $\lambda > 300$ because the configurations exceeded cluster capacity.

studied in [10]. InferLine finds a configuration more than *5x cheaper* than the coarse-grained provisioning (Fig. 7(a)). Both systems achieve near-zero SLO miss rates throughout most of the workload, when the big spike occurs we observe that the InferLine’s reactive controller works as described in §5. As soon as the spike dissipates, InferLine scales the pipeline down to maintain a cost-efficient configuration. In contrast, the coarse-grained reactive controller operates much slower and, therefore, is ill-suited for reacting to rapid changes in the request rate of the arrival process.

In Fig. 7(b), InferLine scales up the pipeline smoothly and recovers rapidly from an instantaneous spike, unlike the CG baseline. Furthermore, as the workload drops quickly after 1000s, InferLine rapidly responds by shutting down replicas to reduce cluster cost. At the end of the workload InferLine and the coarse-grained pipelines converge to similar costs due to the low terminal request rate which hides the effects of pipeline imbalance.

We further evaluate the differences between the InferLine and coarse-grained reactive controllers on a set of synthetic workloads with increasing arrival rates

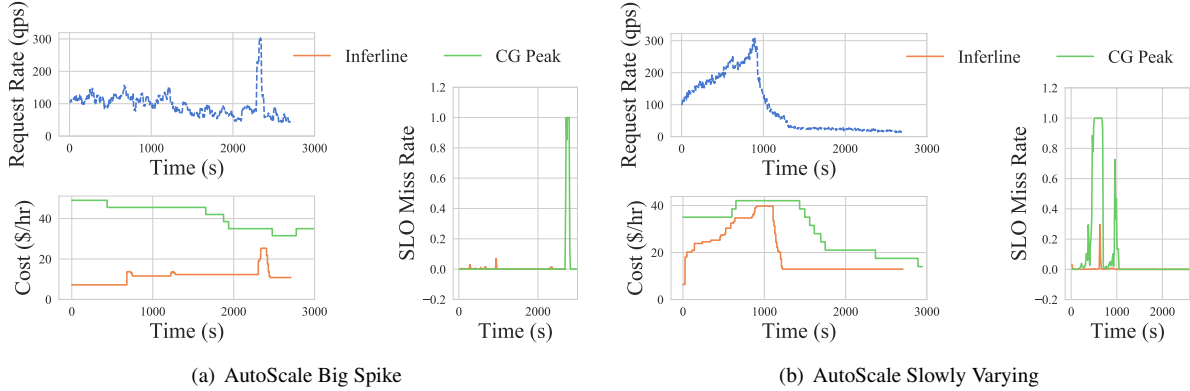


Figure 7: Performance comparison of the reactive control algorithms on traces derived from real workloads. These are the same workloads evaluated in [10] which forms the basis for the coarse-grained baseline.

in Fig. 8. We observe that the arrival curve monitoring described in §5 enables InferLine to detect the increase in arrival rate earlier and therefore scale up the pipeline in time to maintain a low SLO miss rate. In contrast, the coarse-grained reactive controller only reacts to the increase in request rate at the point when the pipeline is overloaded and therefore reacts when the pipeline is already in an infeasible configuration. The effect of this delayed reaction is compounded by the longer provisioning time needed replicate an entire pipeline, resulting in the coarse-grained baselines being unable to recover before the experiment ends. They will eventually recover as we see in Fig. 7 but only after suffering a period of 100% SLO miss rate.

7.2 Sensitivity Analysis

We evaluate InferLine’s sensitivity and robustness in its two major building blocks: its proactive *Planner* and the *Reactive Controller*. We show that the *Planner* is robust to varying arrival rates, latency SLOs, and burstiness factors. For the reactive controller, we analyze InferLine’s sensitivity to changes in the arrival process.

7.2.1 Proactive: Optimizer Sensitivity

InferLine’s *Planner* performs well under varying load, burstiness, and end-to-end latency SLOs. We observe three important trends in Fig. 9. First, increasing burstiness (from CV=1 to CV=4) requires more costly configurations as the optimizer provisions more capacity to ensure that transient bursts do not cause the queues to diverge more than the SLO allows. We see this trend over a range of different arrival throughputs. We also see the cost gap narrowing between CV=1 and CV=4 as the

SLO increases. As the SLO increases, additional slack in the deadline can absorb more variability in the arrival process. Second, the cost generally decreases as a function of the latency SLO, enabling deadline vs. cost tradeoffs at the application level by using InferLine *Planner* to quantify this tradeoff. While this downward cost trend generally holds, the optimizer occasionally finds sub-optimal configurations, as it makes locally optimal decisions to change a resource assignment. Third, the cost increases as a function of expected arrival rate.

7.2.2 Reactive: Arrival Rate Sensitivity

A common type of unpredictable behavior is a change in the arrival rate. We compare the behavior of the system with and without its reactive controller enabled as the arrival process changes from the provisioned 150qps to 250qps. We vary the rate of arrival throughput change τ . InferLine is able to maintain the SLO miss rate close to zero while matching or beating two alternatives: (a) a proactive-only planner given the oracular knowledge of the whole arrival trace a priori, and (b) a proactive-only planner that doesn’t respond to change. Indeed, in Fig. 10, InferLine continues to meet the SLO, and increases the cost of the allocation only for the duration of the unexpected burst. The oracular proactive planner provisions the whole pipeline with the knowledge of the bursty behavior and is equipped with ability to tune all three control knobs (§3.1). The proactive-only planner without oracular knowledge starts missing latency SLOs as soon as the ingest rate increases.

7.2.3 Reactive: Burstiness Sensitivity

A less obvious but potentially debilitating change in the arrival process is an increase in its burstiness, while maintaining the same mean arrival rate. This type of ar-

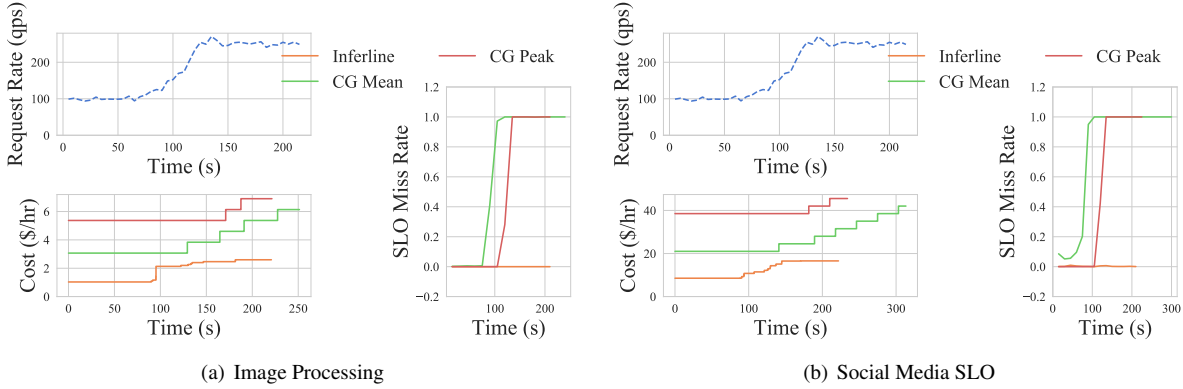


Figure 8: Performance comparison of the reactive control algorithms on synthetic traces with increasing arrival rates.

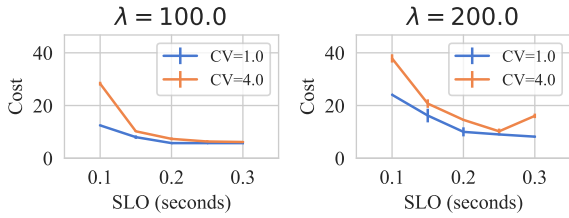


Figure 9: *Planner* sensitivity: Variation in configuration cost across different arrival processes and latency SLOs.

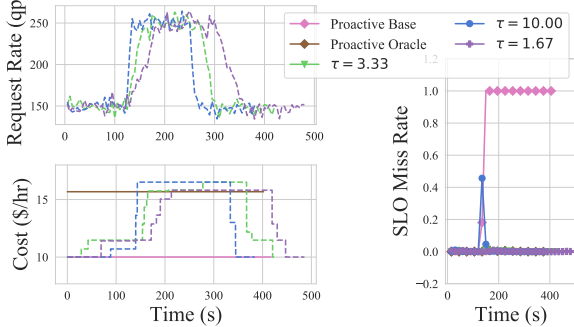


Figure 10: Sensitivity to arrival rate changes.

rival process change is also harder to detect, as the common practice is to look at moments of the distribution, such as the mean or 99th percentile latency. In Fig. 11 we show that InferLine is able to *detect* deviation from expected arrival burstiness and react to meet the latency SLOs.

7.3 Attribution of Benefit

InferLine benefits from (a) fine-grain proactive planning and (b) fine-grain reactive planning. Thus, we evaluate the following comparison points: coarse grain proactive (CG Pro), fine-grain proactive (FG Pro), fine-

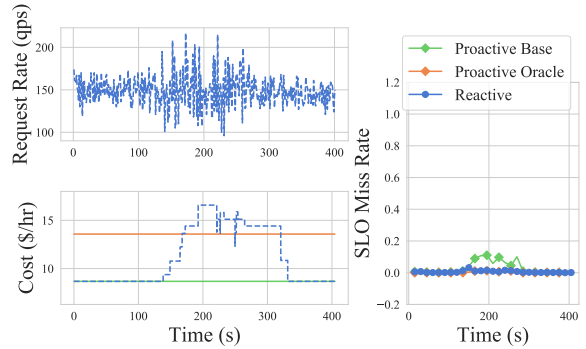


Figure 11: Sensitivity to arrival burstiness changes.

grain proactive with coarse-grain reactive (FG Pro + CG React), and fine-grain proactive with fine-grain reactive (FG Pro + FG React), building up from pipeline-level configuration to the full feature set InferLine provides. Fine-grained proactive planner reduces the cost of the initial pipeline configuration by more than 3x (Fig. 12), but starts missing latency SLOs when the request rate increases. Adding the reactive controller (FG Pro + CG React) adapts the configuration, but too late to completely avoid SLO misses. It recovers faster than proactive-only options. The fine-grain reactive controller meets all SLOs, illustrating the need for both the *Planner* for initial cost-efficient pipeline configuration, and the *Reactive Controller* to promptly and cost-efficiently adapt.

7.4 Generality

The contributions of this work extend generalize to different physical serving engines. Here we layer the InferLine planning and queuing layers on top of TensorFlow Serving (TFS)—a state-of-the-art model serving framework developed at Google. In this experiment, we

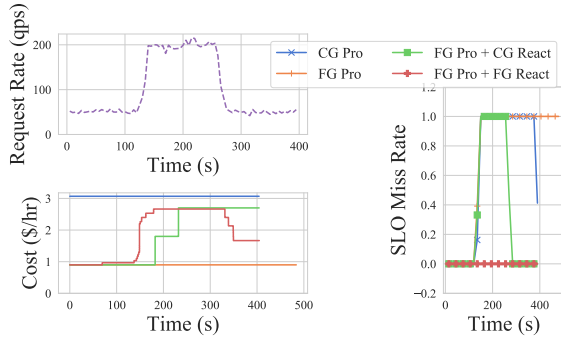


Figure 12: Attribution of benefit between the InferLine reactive and proactive components.

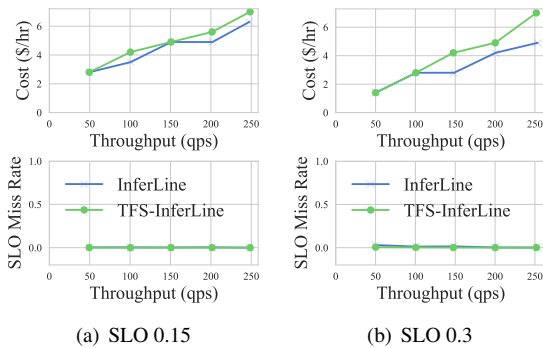


Figure 13: Comparison of InferLine’s planner running on our serving engine and on TensorFlow-Serving.

achieve the same low latency SLO miss rate as InferLine. This indicates the generality of the planning algorithms used to configure individual models in InferLine. In Fig. 13 we show both the SLO attainment rates and the cost of pipeline provisioning when running InferLine on our in-house physical execution engine and on TFS. The cost of the latter is slightly worse due to the additional overhead of TFS RPC serialization. TFS uses gRPC [11] for communication which requires an additional copy of the inputs and outputs of a model, while our serving engine uses an optimized zero-copy RPC implementation.

8 Related Work

A number of recent efforts study the design of generic prediction serving systems [4, 8, 32]. TensorFlow Serving [32] is a commercial grade prediction serving system primarily designed to support prediction pipelines implemented using TensorFlow [31]. Unlike InferLine, TensorFlow Serving adopts a monolithic design with the pipeline orchestration living within a single process. Thus, TensorFlow Serving is able to introduce performance optimizations like operator fusion across

computation stages to reduce coordination between the CPU and GPU at the expense of fine-grain, independent model configuration. Baylor et al. [4] extend TensorFlow-Serving to support the larger machine learning life-cycle, adding more support for basic data transformations and multitenancy in the serving system. However, neither TensorFlow-Serving nor [4] support SLO constraints.

Alternatively, Clipper [8] adopts a more distributed design, similar to InferLine. Like InferLine, each model in Clipper is individually managed, configured, and deployed in a separate Docker container. This design improves isolation across models at the expense of greater data movement. However, Clipper does not directly support prediction pipelines or reasoning about latency deadlines across model composition. It also does not dynamically scale deployments in response to changing workloads.

Mirhoseini et al. [23] use RL to automatically optimize hardware placement for deep learning in heterogeneous hardware environments. However, this work focuses on model placement for training, not prediction serving. These techniques could potentially be extended to prediction serving, but require substantial training.

Zhang et al. [35] explore the design of a streaming video processing system in the VideoStorm project. VideoStorm adopts a distributed design with pipeline operators provisioned across compute nodes and explores the combinatorial search space of hardware and model configurations. However, VideoStorm relies on the pipeline developer to supply their own model configuration control parameters while InferLine automatically determines resource type and batching.

A large body of prior work leverages profiling to inform better scheduling. Workflow-aware scheduling, however, is a relatively recent phenomenon, including SLURM-integrated HPC scheduler published in 2017 [27] and Morpheus [18]. In contrast, InferLine heavily exploits the compute-intensive and side-effect free nature of ML models to estimate end-to-end pipeline performance based on individual model profiles.

Autoscale [10] offers a comprehensive literature review of a body of work aimed at automatically scaling the number of servers reactively, subject to changing load in the context of web services. Autoscale works well for single model replication without batching. It assumes bit-at-a-time instead of batch-at-a-time query processing. We borrow the Autoscale state-of-the-art scaling mechanism for configuring the replication factor for coarse-grain reactive baselines. We find that the

fine-grained reactive control proposed far outperforms the coarse-grain reactive pipeline replication based on Autoscale (§7.1.2).

9 Conclusion

Configuring and serving sophisticated prediction pipelines across heterogeneous parallel hardware while minimizing cost and ensuring SLO attainment presents categorically new challenges in system design. In this paper we introduce InferLine—a system which efficiently provisions and executes prediction pipelines subject to end-to-end latency constraints by proactively optimizing and reactively controlling per-model configurations. We leverage the predictability performance scaling characteristics of machine learning models to enable accurate end-to-end performance estimation and proactive cost minimizing pipeline configuration. In addition, by exploiting the side-effect free, functional nature of machine learning models we are able to *reactively* adapt pipeline configurations to accommodate changes in the query workload. InferLine builds on three main contributions: (a) the fine-grain proactive planning algorithm for pipeline configuration (§4), (b) the fine-grain, robust reactive algorithm to adapt to unexpected changes in load (§5), (c) the SLO- and heterogeneity-aware batched queuing layer of the physical execution engine (§3), to achieve the combined effect of *cost-efficient* heterogeneous inference pipelines that can be deployed to serve applications with a range of tight end-to-end latency objectives. As a result, we achieve up to 7.6x improvement in cost and 32x improvement in SLO attainment for the same throughput and latency objectives over state-of-the-art alternatives.

References

- [1] J. Andreas, M. Rohrbach, T. Darrell, and D. Klein. Deep compositional question answering with neural module networks. *CoRR*, abs/1511.02799, 2015.
- [2] A. Angelova, A. Krizhevsky, V. Vanhoucke, A. S. Ogale, and D. Ferguson. Real-Time Pedestrian Detection with Deep Network Cascades. *BMVC*, pages 32.1–32.12, 2015.
- [3] P. Auer, N. Cesa-Bianchi, Y. Freund, and R. E. Schapire. The nonstochastic multiarmed bandit problem. *SIAM J. Comput.*, 32(1):48–77, Jan. 2003.
- [4] D. Baylor, E. Breck, H.-T. Cheng, N. Fiedel, C. Y. Foo, Z. Haque, S. Haykal, M. Ispir, V. Jain, L. Koc, C. Y. Koo, L. Lew, C. Mewald, A. N. Modi, N. Polyzotis, S. Ramesh, S. Roy, S. E. Whang, M. Wicke, J. Wilkiewicz, X. Zhang, and M. Zinkevich. TFX: A tensorflow-based production-scale machine learning platform. In *Proceedings of the 23rd ACM SIGKDD International Conference on Knowledge Discovery and Data Mining*, KDD ’17, pages 1387–1395. ACM, 2017.
- [5] A. Beck. Simulation: the practice of model development and use. *Journal of Simulation*, 2(1):67–67, Mar 2008.
- [6] L. Breiman. Bagging predictors. *Mach. Learn.*, 24(2):123–140, Aug. 1996.
- [7] L. Breiman, J. H. Friedman, R. A. Olshen, and C. J. Stone. *Classification and Regression Trees*. Statistics/Probability Series. Wadsworth Publishing Company, Belmont, California, U.S.A., 1984.
- [8] D. Crankshaw, X. Wang, G. Zhou, M. J. Franklin, J. E. Gonzalez, and I. Stoica. Clipper: A low-latency online prediction serving system. In *14th USENIX Symposium on Networked Systems Design and Implementation (NSDI 17)*, pages 613–627, Boston, MA, 2017. USENIX Association.
- [9] J. Fowers, K. Ovtcharov, M. Papamichael, T. Massengill, M. Liu, D. Lo, S. Alkalay, M. Haselman, L. Adams, M. Ghandi, S. Heil, P. Patel, A. Sapek, G. Weisz, L. Woods, S. Lanka, S. K. Reinhardt, A. M. Caulfield, E. S. Chung, and D. Burger. A configurable cloud-scale dnn processor for real-time ai. In *Proceedings of the 45th Annual International Symposium on Computer Architecture*, ISCA ’18, pages 1–14, Piscataway, NJ, USA, 2018. IEEE Press.
- [10] A. Gandhi, M. Harchol-Balter, R. Raghunathan, and M. A. Kozuch. Autoscale: Dynamic, robust capacity management for multi-tier data centers. *ACM Trans. Comput. Syst.*, 30(4):14:1–14:26, Nov. 2012.
- [11] GRPC. <https://grpc.io/>.
- [12] J. Guan, Y. Liu, Q. Liu, and J. Peng. Energy-efficient Amortized Inference with Cascaded Deep Classifiers. *arXiv.org*, Oct. 2017.

- [13] K. He, X. Zhang, S. Ren, and J. Sun. Deep residual learning for image recognition. *arXiv preprint arXiv:1512.03385*, 2015.
- [14] A. W. S. Inc. Amazon sagemaker: Developer guide. <http://docs.aws.amazon.com/sagemaker/latest/dg/sagemaker-dg.pdf>, 2017.
- [15] Y. Jia, E. Shelhamer, J. Donahue, S. Karayev, J. Long, R. Girshick, S. Guadarrama, and T. Darrell. Caffe: Convolutional architecture for fast feature embedding. In *Proceedings of the ACM International Conference on Multimedia*, pages 675–678. ACM, 2014.
- [16] M. J. Jones and P. Viola. *Robust real-time object detection*. Workshop on Statistical and Computational Theories . . . , 2001.
- [17] N. P. Jouppi, C. Young, N. Patil, D. Patterson, G. Agrawal, R. Bajwa, S. Bates, S. Bhatia, N. Boden, A. Borchers, R. Boyle, P.-I. Cantin, C. Chao, C. Clark, J. Coriell, M. Daley, M. Dau, J. Dean, B. Gelb, T. V. Ghaemmaghami, R. Gottipati, W. Gulland, R. Hagmann, C. R. Ho, D. Hogberg, J. Hu, R. Hundt, D. Hurt, J. Ibarz, A. Jaffey, A. Jaworski, A. Kaplan, H. Khaitan, D. Killebrew, A. Koch, N. Kumar, S. Lacy, J. Laudon, J. Law, D. Le, C. Leary, Z. Liu, K. Lucke, A. Lundin, G. MacKean, A. Maggiore, M. Mahony, K. Miller, R. Nagarajan, R. Narayanaswami, R. Ni, K. Nix, T. Norrie, M. Omernick, N. Penukonda, A. Phelps, J. Ross, M. Ross, A. Salek, E. Samadiani, C. Severn, G. Sizikov, M. Snellham, J. Souter, D. Steinberg, A. Swing, M. Tan, G. Thorson, B. Tian, H. Toma, E. Tuttle, V. Vasudevan, R. Walter, W. Wang, E. Wilcox, and D. H. Yoon. In-datacenter performance analysis of a tensor processing unit. In *Proceedings of the 44th Annual International Symposium on Computer Architecture*, ISCA '17, pages 1–12, 2017.
- [18] S. A. Jyothi, C. Curino, I. Menache, S. M. Narayana-murthy, A. Tumanov, J. Yaniv, R. Mavlyutov, I. n. Goiri, S. Krishnan, J. Kulkarni, and S. Rao. Morpheus: Towards automated slos for enterprise clusters. In *Proceedings of the 12th USENIX Conference on Operating Systems Design and Implementation*, OSDI'16, pages 117–134, Berkeley, CA, USA, 2016. USENIX Association.
- [19] J.-Y. Le Boudec and P. Thiran. *Network Calculus: A Theory of Deterministic Queuing Systems for the Internet*. Springer-Verlag, Berlin, Heidelberg, 2001.
- [20] L. Li, W. Chu, J. Langford, and R. E. Schapire. A contextual-bandit approach to personalized news article recommendation. In *WWW*, 2010.
- [21] M. Malinowski, M. Rohrbach, and M. Fritz. Ask your neurons: A neural-based approach to answering questions about images. *2015 IEEE International Conference on Computer Vision (ICCV)*, pages 1–9, 2015.
- [22] M. McGill and P. Perona. Deciding How to Decide: Dynamic Routing in Artificial Neural Networks. *arXiv.org*, Mar. 2017.
- [23] A. Mirhoseini, H. Pham, Q. Le, M. Norouzi, S. Bengio, B. Steiner, Y. Zhou, N. Kumar, R. Larsen, and J. Dean. Device placement optimization with reinforcement learning. 2017.
- [24] Open ALPR. <https://www.openalpr.com/>.
- [25] A. Paszke, S. Gross, S. Chintala, G. Chanan, E. Yang, Z. DeVito, Z. Lin, A. Desmaison, L. Antiga, and A. Lerer. Automatic differentiation in pytorch. 2017.
- [26] J. Redmon, S. Divvala, R. Girshick, and A. Farhadi. You only look once: Unified, real-time object detection. In *Proceedings of the IEEE conference on computer vision and pattern recognition*, pages 779–788, 2016.
- [27] G. P. Rodrigo, E. Elmroth, P.-O. Östberg, and L. Ramakrishnan. Enabling workflow-aware scheduling on hpc systems. In *Proceedings of the 26th International Symposium on High-Performance Parallel and Distributed Computing*, HPDC '17, pages 3–14, New York, NY, USA, 2017. ACM.
- [28] D. Sculley, G. Holt, D. Golovin, E. Davydov, T. Phillips, D. Ebner, V. Chaudhary, and M. Young. Machine learning: The high interest credit card of technical debt. In *SE4ML: Software Engineering for Machine Learning (NIPS 2014 Workshop)*, 2014.
- [29] E. Sparks. *End-to-End Large Scale Machine Learning with KeystoneML*. PhD thesis, EECS Department, University of California, Berkeley, Dec 2016.
- [30] Y. Sun, X. Wang, and X. Tang. Deep Convolutional Network Cascade for Facial Point Detection. *CVPR*, pages 3476–3483, 2013.
- [31] TensorFlow. <https://www.tensorflow.org>.
- [32] TensorFlow Serving. <https://tensorflow.github.io/serving>.
- [33] X. Wang, Y. Luo, D. Crankshaw, A. Tumanov, and J. E. Gonzalez. IDK cascades: Fast deep learning by learning not to overthink. *CoRR*, abs/1706.00885, 2017.
- [34] Y. Yang, D.-C. Zhan, Y. Fan, Y. Jiang, and Z.-H. Zhou. Deep learning for fixed model reuse, 2017.
- [35] H. Zhang, G. Ananthanarayanan, P. Bodik, M. Philipose, P. Bahl, and M. J. Freedman. Live video analytics at scale with approximation and delay-tolerance. In *14th USENIX Symposium on Networked Systems Design and Implementation (NSDI 17)*, pages 377–392, Boston, MA, 2017. USENIX Association.